



Modeling of Rayleigh waves dispersion in the Sannio region (Southern Italy) from seismic active refraction data

Salvatore de Lorenzo^{1,*}, Giovanni Iannaccone² & Aldo Zollo³

¹Dipartimento di Geologia e Geofisica, Università di Bari, Italy; ²Osservatorio Vesuviano, Ercolano, Napoli, Italy; ³Dipartimento di Scienze Fisiche, Università di Napoli, Italy; *for correspondence: e-mail: delorenzo@geo.uniba.it

Received 11 July 2000; accepted in revised form 25 January 2002

Key words: complete wave field, dispersion, group velocity, Rayleigh waves, Sannio, semblance, synthetic seismograms

Abstract

Short period surface waves, recorded during a seismic refraction survey in the Sannio region (Southern Italy), have been modeled to infer a shallow velocity model for the area. Based on the decrease of resolution with depth, due to the bias on group velocity estimates arising from interference of the Rayleigh waves with higher modes, we carried out a procedure of fitting, with synthetic seismograms, of selected filtered traces with a gaussian filter, having a width at half height equal to 1 Hz and a central frequency lying in the range [1,4] Hz. We estimated the likelihood between synthetic and observed seismograms by measuring their semblance. In this way we were able to infer a more refined local velocity model characterized by a high V_p and V_s vertical gradient in the sedimentary cover. Two ad hoc resolution studies, based on group velocity and amplitude data respectively, indicate that the local velocity model is a good velocity model also for the entire studied area. The increase in the number of available data when using amplitude information allows us to make a more selective choice in the model parameter space (V_p and V_s of each layer) and to solve for the V_p/V_s ratio. The inferred V_p velocity in the half-space is equal to 2.8 km/s. This value is in excellent agreement with that inferred by other authors (3 km/s) by modeling P-wave travel time vs. distance. The best-fit model furnish low V_p/V_s for the sedimentary cover so indicating a high degree of the sediment's compaction in the studied area. The inferred shallow high-velocity gradient indicates that the shallow sedimentary layer in the area could trap and focus the energy traveling into it.

Introduction

In the last two decades substantial improvements have been made in simulating the propagation of the complete wave field in elastic and anelastic flat layer structures. The matching between the discrete wave-number method (Bouchon, 1979, 1981) and the classical propagator matrix methods (Harkrider, 1964; Dunkin, 1965; Kennett, 1983) allows, actually, for adequately computing the complete wave field generated by a point-like, or extended, seismic source, embedded in an elastic (or anelastic) medium formed by an assigned number of flat layers.

The relevant theoretical progresses reached in site effects study (see e.g. Bard and Bouchon, 1985)

clearly indicate the fundamental role played by the elastic properties of the surface sedimentary layers on site amplification. These studies motivate the actual effort of many experimental researches aimed at obtaining detailed images of the V_p and V_s variations of the shallow sedimentary layers overlying the bedrock (e.g. Malagnini et al., 1997). Usually the very shallow structure is reconstructed with ad hoc small scale experiments using seismic reflection or refraction survey.

During October 1992 an active seismic refraction survey was performed in Southern Apennine (Italy). The main aim of the experiment was the determination of a P wave velocity model for the upper crust in the Sannio region (Iannaccone et al., 1998). The

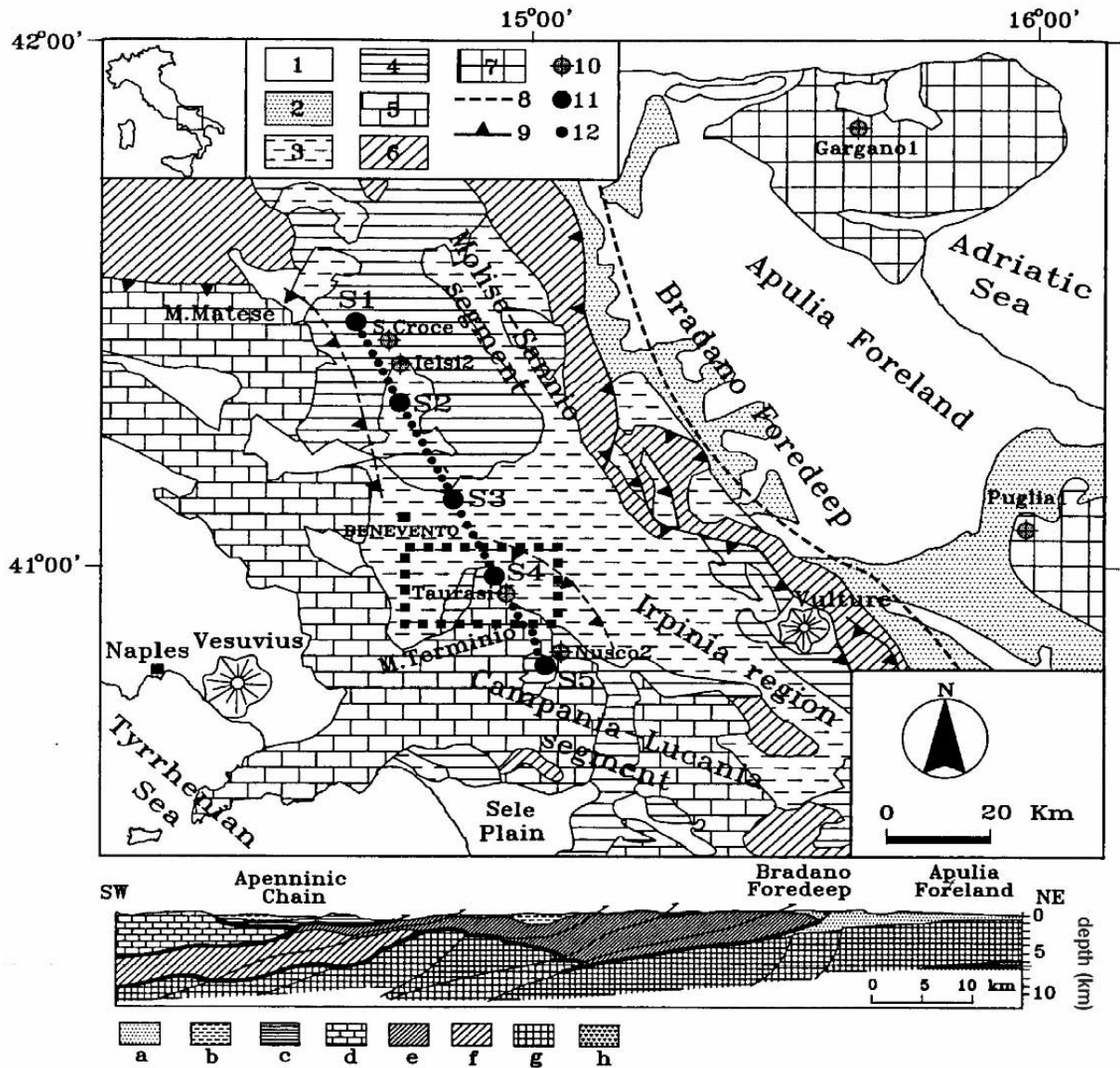


Figure 1a. Simplified geological sketch of the Southern Apennines. 1 – Middle-Upper Pleistocene and Holocene deposits; 2 – Upper Pliocene-Lower Pleistocene deposits; 3 – Upper Tortonian to Upper Pliocene thrust-sheets-top deposits; 4 – Sannio and Sicilide Nappes (Paleogene-Lower Miocene); 5 – Western Carbonate Platform (Mesozoic Tertiary) and unconformable Upper Miocene siliciclastic flysch deposits of the related marginal areas; 6- Lagonegro and Molise Basin sequences (Mesozoic Tertiary); 7 – Apulia Carbonate Platform (Mesozoic Tertiary); 8 – buried frontal ramp of the Apennine thrust sheets; 9 – out of sequence thrust; 10 – well; 11 – shot point; 12 – seismic stations. Schematic geological cross section of the Northern sector of the Southern Apennines. (a) Plio-Pleistocene deposits of the Bradano foredeep; (b) Later Tortonian to Upper Pliocene thrust-sheets-top deposits; (c) Sannio nappe (Paleogene-Lower Miocene); (d) Western Carbonate Platform (Mesozoic Tertiary) and unconformable Upper Miocene flysch deposits of the related marginal areas; (e) Lagonegro and Molise Basin upper sequences (Cenozoic); (f) Lagonegro and Molise Basin lower sequences (Mesozoic); (g) Apulia Carbonate Platform (Mesozoic Tertiary); (h) Verrucano formation (Permian-Lower Triassic). The shaded rectangular area represents the zone considered in this study. (after Improta et al., 2000).

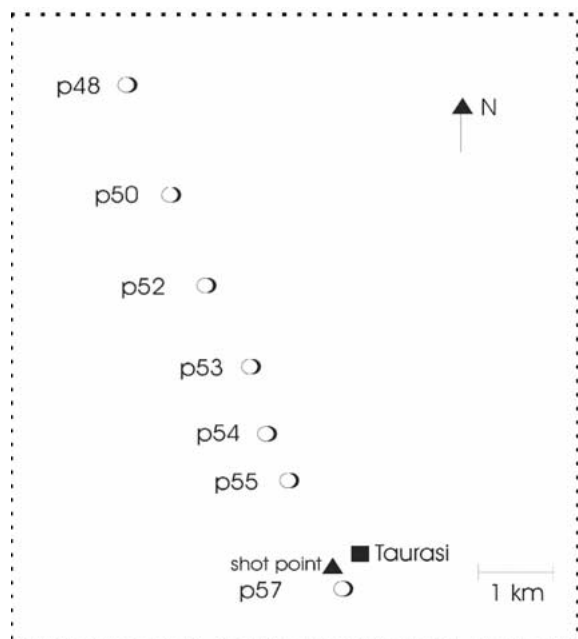


Figure 1b. Zoom of the rectangular shaded area of Figure 1a, to obtain a visible image of the geometrical disposition of the shot point and the seismic stations considered in this study.

experiment was performed in the framework of a multidisciplinary research program supported by the European Community to develop a microzonation and hazard methodology to be applied to Benevento, the main town of the Sannio area.

The Sannio region has been struck by strong earthquakes in historical times ($I_0 > X$ MCS), as inferred from intensity data. At present time, the seismicity of this region is characterized by low energy earthquakes, clustered in swarms that indicate seismic activity occurring at the borders of seismogenetic zones which caused the most energetic earthquakes (Iannaccone et al., 1998).

In this framework, the knowledge of the very shallow structure of the region is of fundamental interest both in the evaluation of site amplification effects, in the relocation of earthquakes foci, and in the calculation of accurate fault plane solutions.

In this paper we use data recorded during the 'Benevento 92' seismic refraction experiment, performed at regional scale to obtain a structural model of the upper crust, to reproduce the elastic properties of surface sedimentary layers. At this aim a surface waveform modeling technique, based on fitting of filtered traces, has been applied to analyze the short period surface waves produced by artificial sources.

Data and techniques

In our analysis we considered some selected seismograms recorded during a seismic refraction experiment conducted in the Sannio region (Southern Italy). It consisted in six shots ranging from 400 to 600 kg fired at five sites equally spaced along a line of 75 km long (Figure 1a). Each shot was recorded by 71 portable seismic stations placed along the seismic line. All the seismic stations were equipped with short period seismometer with a natural frequency of 1 or 2 Hz. A detailed description of the experiment can be found in Iannaccone et al., (1998). The recorded data were interpreted by Improta et al. (2000) using a 2-D ray-tracing technique constraining the interpretation of the seismic model by stratigraphic and sonic velocity logs from well oil exploration. The obtained crustal velocity model shows a surface layer interpreted as cenozoic flyschoid cover and basinal successions with a mean thickness of 1.5 km and P-wave velocity of about 3–3.3 km/s. A second layer with a P-wave velocity of 4.8 km/s interpreted as mesozoic basinal sequences overlaying the multilayer carbonate platform with a P-wave velocity of 6.2–6.6 km/s. At greater depth (9.5–11 km) a lower P-wave velocity is hypothesized.

From the available data we selected seismograms showing the clearest and most complete dispersion data. We used records of shot N.4 reported in Improta et al. (2000) performed on the October 10, 1992, by 560 kg of explosive detonated in holes of a maximum depth of 45 m (Figure 1b). By a first inspection of the band-pass filtered traces in the 1–10 Hz frequency range we inferred a highly energetic contribution of the low-frequency Rayleigh waves that follows the higher frequency body waves (Figure 2).

In order to retrieve a preliminary surface velocity model we analyzed the travel times of the first P-wave at the closest stations (Figure 3). The travel times graph can be interpreted with a simple seismic model: a thin surface layer overlaying a half space media with a highest V_p (3300 m/s) value; however, based on the layout of the October 1992 seismic experiment, there is no resolution for such shallow depth analysis by the inversion of the travel time of direct and/or reflected and converted phases recorded during the experiment. From Figure 3 we can only estimate a maximum thickness of the first layer of about 150 m.

A classic way to infer the elastic properties of this surface body can be provided by the modeling of the dispersion curves of group and phase velocity of

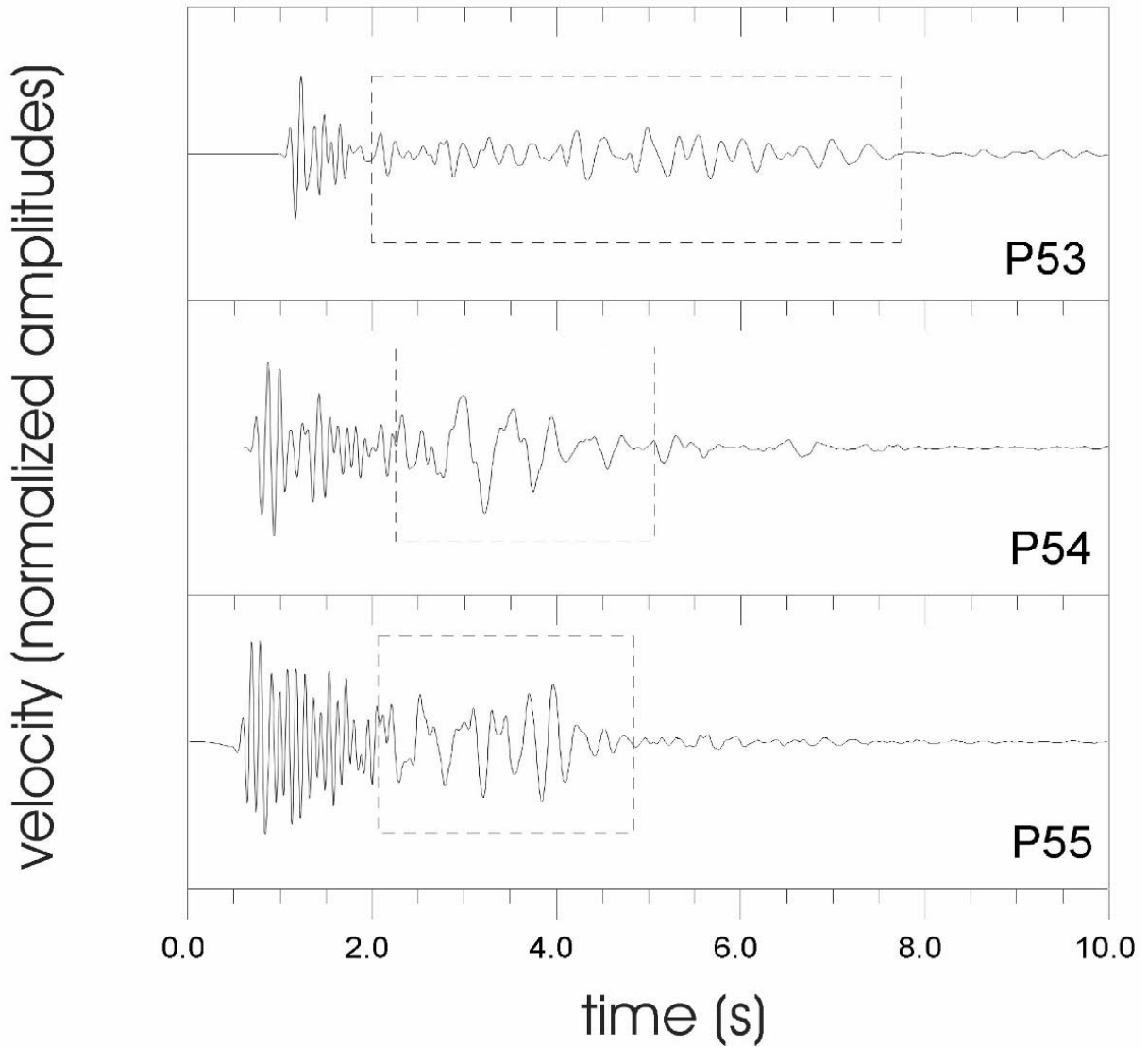


Figure 2. Application of a band-pass filter (1–10) Hz to some traces recorded during the experiment. It is enhanced the contribution of the Rayleigh surface waves (rectangular area) to the wave field generated by the explosive charge.

short period (1–6 Hz) Rayleigh waves generated by the explosion.

Our analysis concerned the modeling of the group velocity vs. frequency data by using a standard classical technique aimed to measure group velocity $U(f_c)$ at a fixed frequency f_c (Dziewonski and Hales, 1972). It consists of the application of a gaussian bandpass filter to the seismogram; the filter function can be expressed in the frequency domain by:

$$H(f) = \begin{cases} e^{-\frac{\pi^2(f-f_c)^2}{\alpha^2}} & 0 \leq f \leq f_c \\ 0 & f \geq f_c \end{cases} \quad (1)$$

where f is the frequency, f_c is the central frequency and α the frequency window around f_c .

It has been shown (Dziewonski and Hales, 1972) that the signal resulting by the application of the filter function (1) to a unimodal wave reaches its maximum value at a time corresponding to the arrival time t^* of the group around the frequency f_c , so that the group velocity is:

$$U(f) = \frac{R}{t^*} \quad (2)$$

with R representing the shot-receiver distance. The filter function (1) could introduce systematic errors

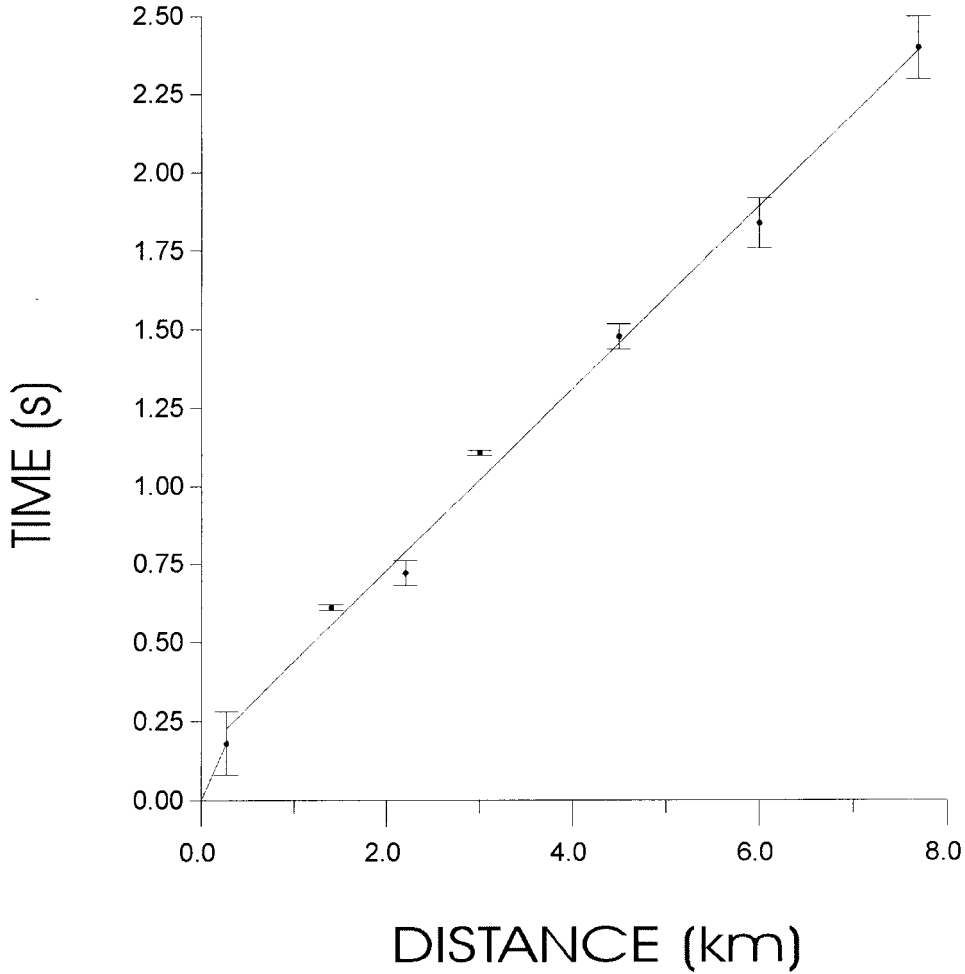


Figure 3. Travel time vs. distance for the profile shown in Figure 1b). The different slope of the straight line interpolating the experimental points at short distance with respect to that interpolating the experimental points at long distances can be interpreted as due to a high V_p velocity gradient in the uppermost crust.

when the medium is strongly dispersive (i.e. group velocity rapidly varies with frequency); in this case the error can be reduced by increasing α , with an increase in the degree of uncertainty on the velocity estimate and the risk of the interference between adjacent modes (Dziewonski and Hales, 1972). Based on this difficult, we carried out a detailed analysis of the effect of the application of the gaussian band-pass filter to the considered traces and discarded data for which a significant bias in the group velocity estimates could arise from interference of time-adjacent modes. The selection of group velocity dispersion data was carried out by means of a seismic data analysis package for digital processing, and only the most energetic

mode, the fundamental mode of the Rayleigh waves, was estimated. In order to measure the uncertainty on group velocity we utilized the relationship:

$$\Delta U = \left| \frac{\partial U}{\partial t^*} \right| \Delta t^* \quad (3)$$

being Δt^* estimated by the half-period of the first sinusoid centered around t^* . Group velocity dispersion data and related uncertainties are shown in Figure 4.

During the collection of the data the major difficult we experienced consisted in extracting information at low frequencies, at about 1 Hz, mainly due to the interference of the Rayleigh waves and the body waves traveling the deep layer. This effect produces in an increase of the difference between estimates of $U(f)$

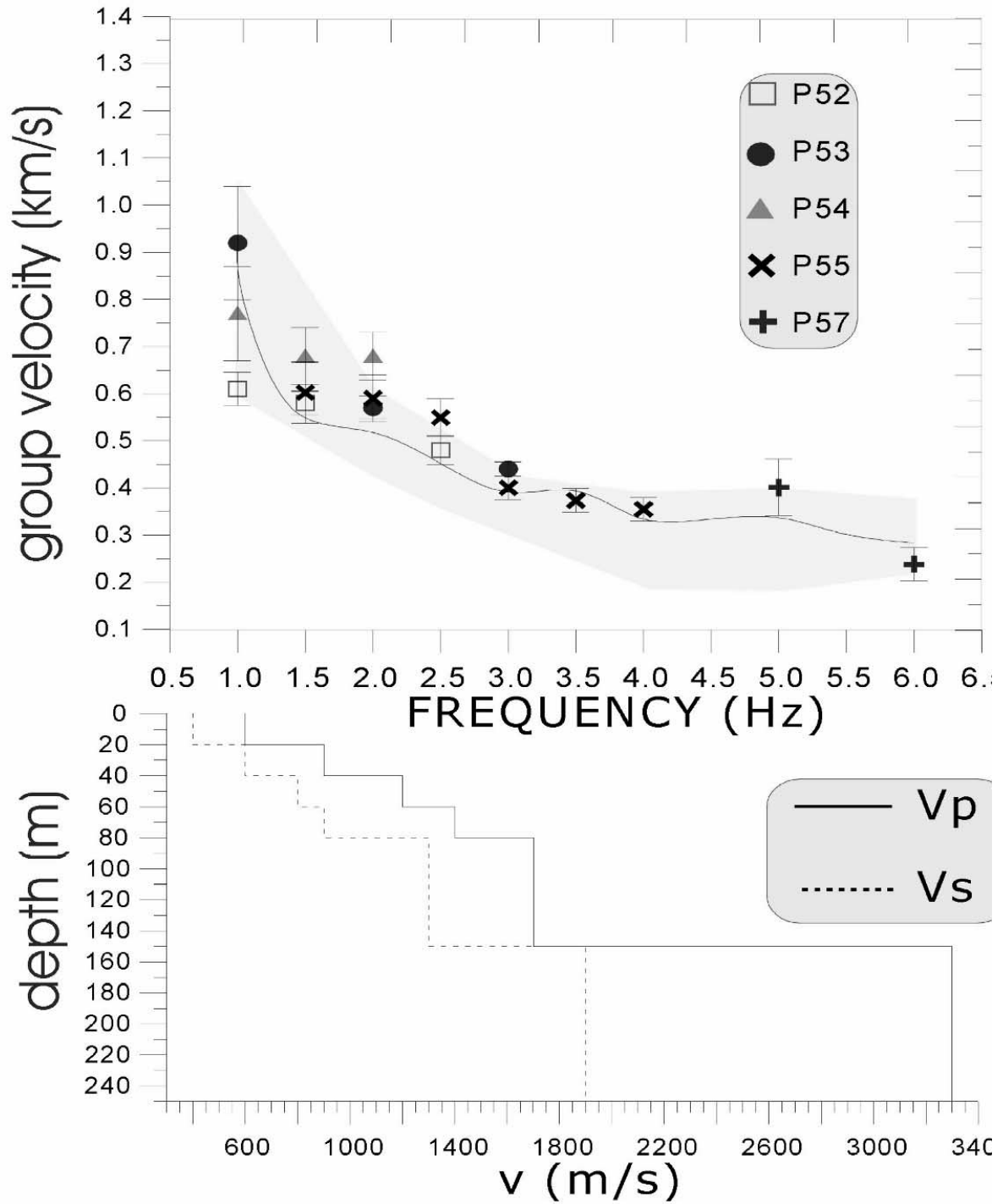


Figure 4. (a) – Modeling of the fundamental mode of group velocity dispersion data. The data and their uncertainties are inferred by the application of a gaussian filter to the original traces. The shaded area quantify the sensitivity of the inferred model to variations in V_p and V_s velocities. The upper and lower limit of this area correspond to variations in body wave velocities equal to ± 0.1 km/s. (b) – The velocity model inferred by the modeling (Table 1).

Table 1. ‘Starting’ velocity model

depth of the top (m)	Vp(m/s)	Vs(m/s)	density (g/cm ³)
0	600.0	400.	2.1
20.	900.0	600.	2.1
40.	1200.	800.	2.1
60.	1400.	900.	2.1
80.	1700.	1300.	2.1
150.	3300.	1900.	2.3

at different stations with decreasing f . Based on this, some data were discarded and only those characterized by a minor level of bias, due to the interference with higher modes, were considered. A decrease of group velocity data with the increasing of the frequency can be deduced by Figure 4.

Modeling of the group velocity dispersion data

Knopoff (1961) firstly observed that determining model layering from the seismic observation, a process known as inverse modeling, tends to give non unique results.

Given the non-uniqueness of solution several efforts have been made to develop inversion techniques based on the local linearization of a misfit function (e.g. Nolet, 1990) or global, non linear procedures based on genetic algorithms (Sambridge and Drijkoningen, 1992) or techniques by using differential seismograms (Du and Foulgers, 1999).

We followed the approach to the problem proposed by Yao and Dorman (1992) that used a forward, rather than inverse, modeling method to infer a layered structure of central and Eastern Tennessee; their technique consists of computing theoretical group velocity dispersion curves by solving the period equation of the Rayleigh waves for a given layered medium via the propagator matrix method (Haskell, 1953; Harkrider, 1964; Dunkin, 1965).

In this paper we used a similar approach, computing the complete wave field to solve for the reflectivity layer matrix representing the period or dispersion equation (Kennett, 1983; Muller, 1985).

In order to simulate the Vp velocity gradient of the shallow layer we subdivided the 1D model in six different layers (5 layer on a halfspace). The initial velocity model was inferred by determining the best fit value of the Vp vertical gradient in a 1D medium

that fits the observed P waves travel times, shown in Figure 3. This was achieved by applying the theory of ray propagation (Lee and Stewart, 1981) in a 1D elastic media. We fixed the density of the first five layers equal to 1.9 g/cm³ and that of the halfspace to 2.3 g/cm³, as derived by preexisting geophysical and geological investigations (Improta et al., 2000). Also we fixed the depth of each interfaces separating the different layers. This model was successively refined through a trial and error perturbative procedure based on fitting of group velocity dispersion data. In this way we were able to infer a theoretical dispersion curve that adequately fits the data (Figure 4a), corresponding to the Vp and Vs velocity model shown in Figure 4b and reported in Table 1 (in the next referred as the starting model).

Also we studied the sensitivity of the inferred model to Vp and Vs variation of each layer. In Figure 4a the shaded area delimitates the range of variation of the theoretical dispersion curve corresponding to variations of Vp and Vs velocities in the range ± 0.1 km/sec.

Overall, the less constrained parameter was the depth of the top of the halfspace (between 100 and 200 m of depth). This is clearly the effect of the previously described large uncertainties affecting data around 1 Hz.

Modeling of the filtered seismograms

In order to better detail the shallow sedimentary structure of the area in the following we considered only the area between the receiver P54 and P55 (Figure 1b). The effect of the application of the gaussian filter, for different values of the central frequency f_c , to the velocigrams recorded at these stations is shown in Figure 5. Only those traces for which there is no overlapping between adjacent modes were considered. Synthetic seismograms have been computed by means of AXITRA, a computer program that implements the discrete wave-number Bouchon’s (1981) theory in conjunction with the reflectivity method (Kennett, 1983). The effect of the explosion was simulated by considering as seismic source an instantaneous, point-like isotropic source, i.e. a Dirac delta function both in the time and in the space domain.

These traces were compared with the corresponding filtered synthetic seismograms obtained by considering as velocity model the previously inferred Vp and Vs velocity model (starting model). Both data and syn-

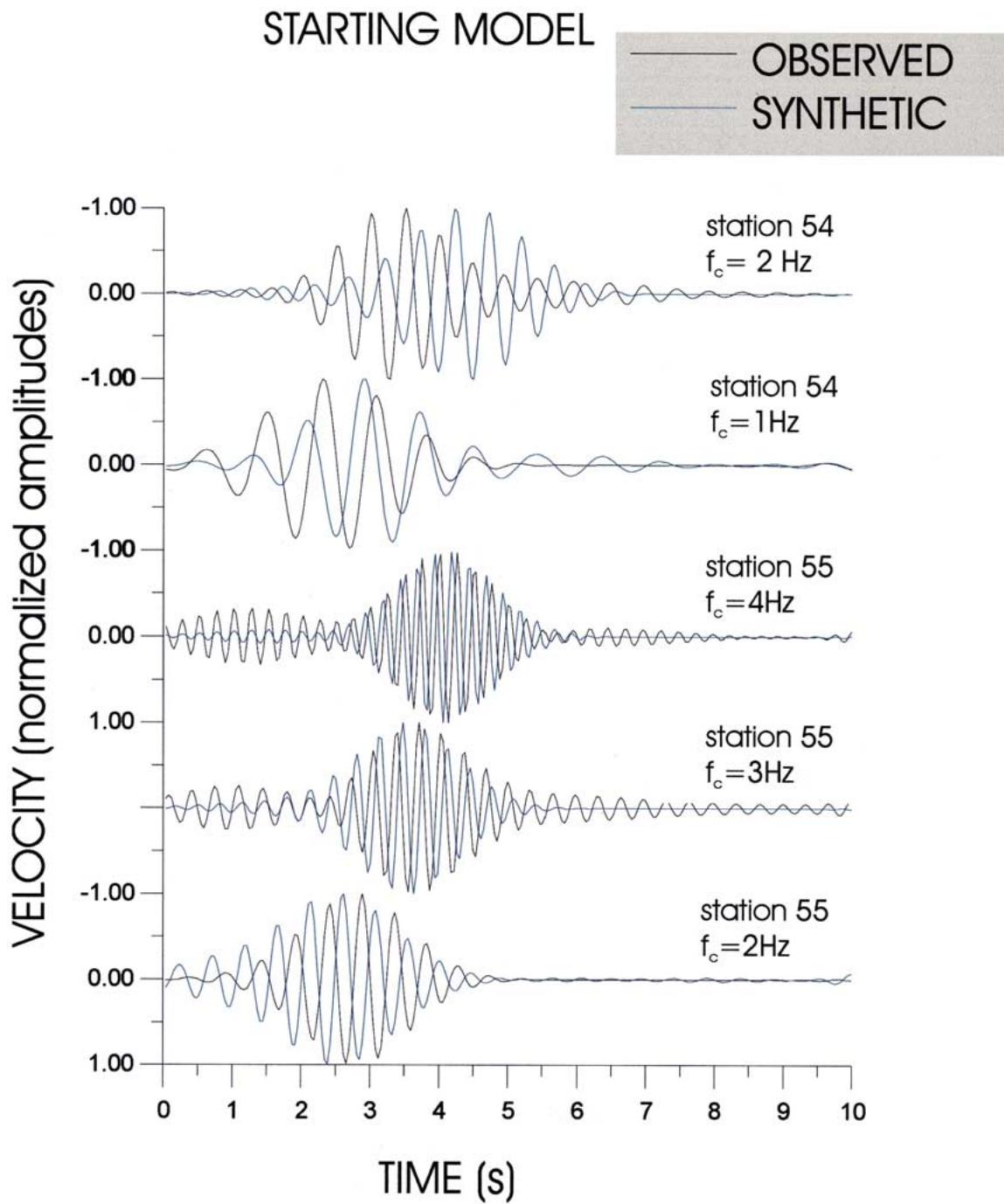


Figure 5. Comparison between the observed gaussian-filtered seismograms (black line) and corresponding synthetic filtered traces (blue line). The velocity model used to compute the synthetic wave field is the starting model (see the text).

Table 2. 'Final' velocity model

depth of the top (m)	Vp (m/s)	Vs (m/s)	density (g/cm ³)	Vp/Vs
0	620.	405.	2.05	1.53
20.	905.	560.	2.28	1.61
40.	1170.	740.	2.00	1.58
60.	1365.	910.	2.10	1.50
80.	1690.	1320.	2.2	1.28
150.	2800.	2200.	2.3	1.27

thetic were digitized at the same rate of sampling and normalized to the unity, due to the lack of amplitude information of the data.

A simple way to quantify the degree of similarity between M seismograms $u_n(t)$ ($1 < n \leq M$) in the time domain t , consists of measuring the semblance S_t defined as (Telford et al., 1990):

$$S_t = \frac{1}{M} \frac{\left[\sum_{n=1}^M \sum_{i=1}^L u_n(t_i) \right]^2}{\sum_{n=1}^M \sum_{i=1}^L u_n^2(t_i)}$$

where $T = t_1 + \dots + t_L$ is the time window considered in the analysis.

For the starting model and the 10 filtered traces deployed in Figure 5 the semblance is equal to 0.154. In order to better detail the elastic properties of the area between P54 and P55 stations we followed a simple approach that consists in progressively adjusting model parameters (Vp, Vs and density of each layer) by optimizing the semblance between the gaussian filtered observed and corresponding synthetic traces. In this way we determined a more detailed local velocity model (Table 2) for the area between P54 and P55 stations. In Figure 6.A,B,C is shown the progressive increase of the semblance after the various refining of the velocity model. The final value of the semblance was 0.205 with a percentage of 35% of increase with respect to the starting model. A high sensitivity of the semblance to variations of model parameters arises from a visual inspection of results of Figure 6. As we will detail in the next sections, we think that this follows from the use of all data constituting the filtered traces that allows us for a more refined search in the model parameter space; physically, we are requiring that our model will reproduce, although locally, not only the time arrivals of narrow frequency-band wave-packets but also their shapes (that is other than fitting

velocity we search to adjust also for the energy content of these packets).

The major difference between the starting and the final model is represented by the body wave velocities of the half-space, whereas the body waves velocities of the intermediate layers result only poorly changed. The comparison between data and filtered traces corresponding to the final velocity model is shown in Figure 7.

Resolution study

The approach proposed in the previous section uses one iteration of the Powell's optimization method (Press et al., 1989), i.e. perturbatively adapting one variable at time. Given the local nature of the obtained maximum of semblance, a resolution analysis is needed in order to clarify at least two aspects. The first consists of establishing if the model so obtained can be considered as a good velocity model for the entire area, i.e. if it corresponds to a minimum misfit value between observed and theoretical group velocity data.

The second consists of establishing what is the level of resolution of model parameters; in particular it is needed to evaluate if the velocity gradient in the shallow layer and the Vp/Vs ratio are effectively resolved or not.

Based on this, in the next two sections we discuss the resolution of the obtained Vp and Vs velocity models and the uncertainties affecting model parameters. Two different resolution analyses have been carried out. In the first we used only group velocity data, in the second the amplitude data (i.e. the entire filtered seismograms) of the five previous considered filtered traces.

a) Group velocity data

A first way to evaluate the resolution of model parameter and their uncertainties consists of representing the misfit between group velocity data and corresponding estimates as a function of model parameters. In this first analysis we used all group velocity data (i.e. between P52 and P57 stations). The calculations were performed for different values of the body wave velocity of each layer around the Vp and Vs values of the obtained velocity model (Table 2). Results are shown in Figure 8. The dashed line in each graph represents the average 1σ standard deviation as inferred by the standard deviations of group velocity data, estimated through the equation (3).

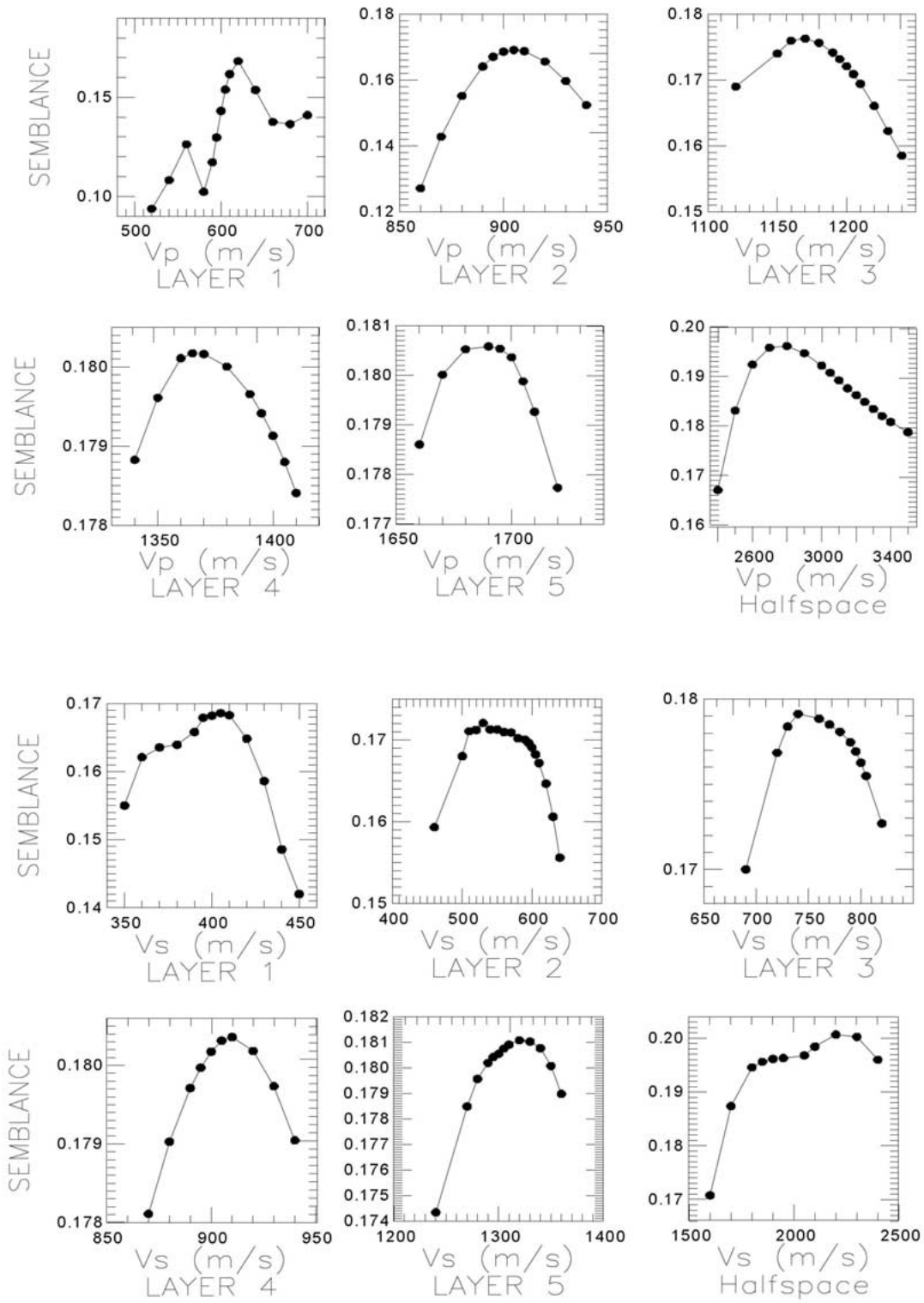


Figure 6.

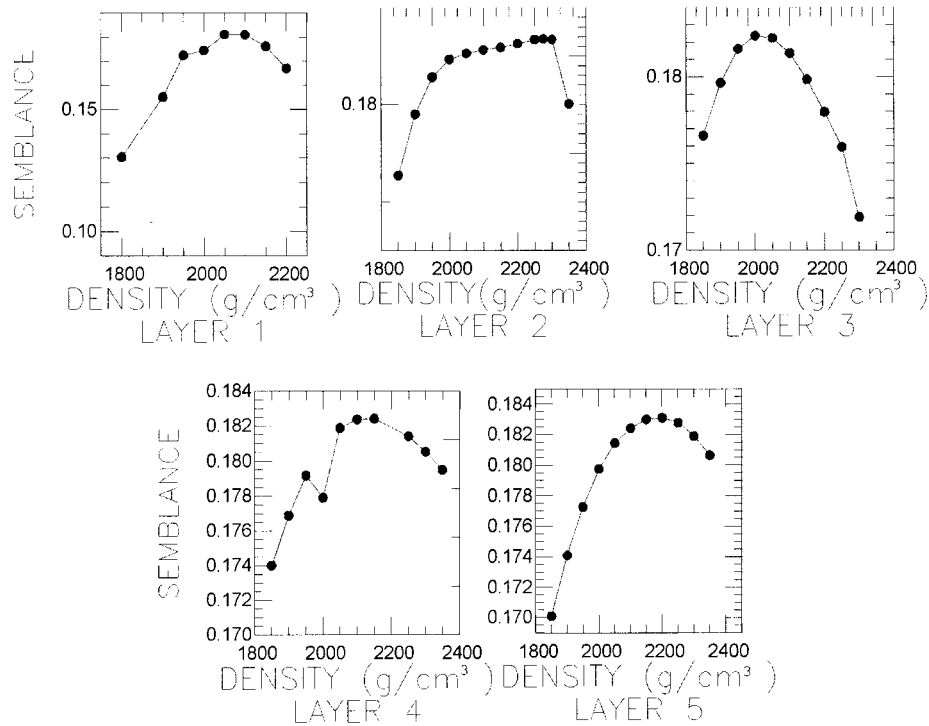


Figure 6. Analysis of sensitivity of the final model. (a) – Variation of the semblance between filtered data and synthetic as a function of the variation of the Vp body velocity in each of the layer. (b) – The same as in (a) but for Vs waves of each layer. (c) – The same as in (a) but for the density of each layer.

Results of Figure 8 indicate that our final model (Table 2), obtained by locally refining the semblance between filtered and synthetic seismograms, represents a good velocity model for the entire studied area, since the minimum value of the misfit function is obtained for Vp and Vs values very close to the Vp and Vs values of the final model (Table 2).

A simple estimate of velocity uncertainties could be obtained by measuring the range of velocity values for which the misfit function is less than the threshold value (the dashed line in Figure 8). If we adopt this criterion we obtain the following results:

1. Vp resolution progressively decreases with increasing depth, with the exception of Vp of layer 5.
2. Vs resolution progressively decreases with decreasing depth, with the exception of Vs of layer 5.
3. Vs is better resolved than Vp in each of the considered layers.

The uncertainties of resolved Vp and Vs model parameters are however very high. This would imply that

we are not able to retrieve the gradient velocity in the shallow layer (depth < 150 m) by using only group velocity data.

However, there is a great discrepancy between the high sensitivity of the semblance to Vp and Vs variations (Figure 6) and the poor resolution arising from the analysis described in Figure 8. This discrepancy is only apparent as we will motivate in the next section.

b) Amplitude data

By the observed filtered traces, used in the semblance analysis, we can obtain a simple estimate of uncertainties on amplitudes by using the error propagation formula:

$$\Delta A = \frac{1}{N} \sum_{i=1}^N \left| \frac{\partial A_i}{\partial t} \right| \Delta t$$

where Δt is the sampling time and N the number of considered point in the seismogram. Averaging on the five filtered traces, and discarding amplitude data whose absolute value is below a given threshold

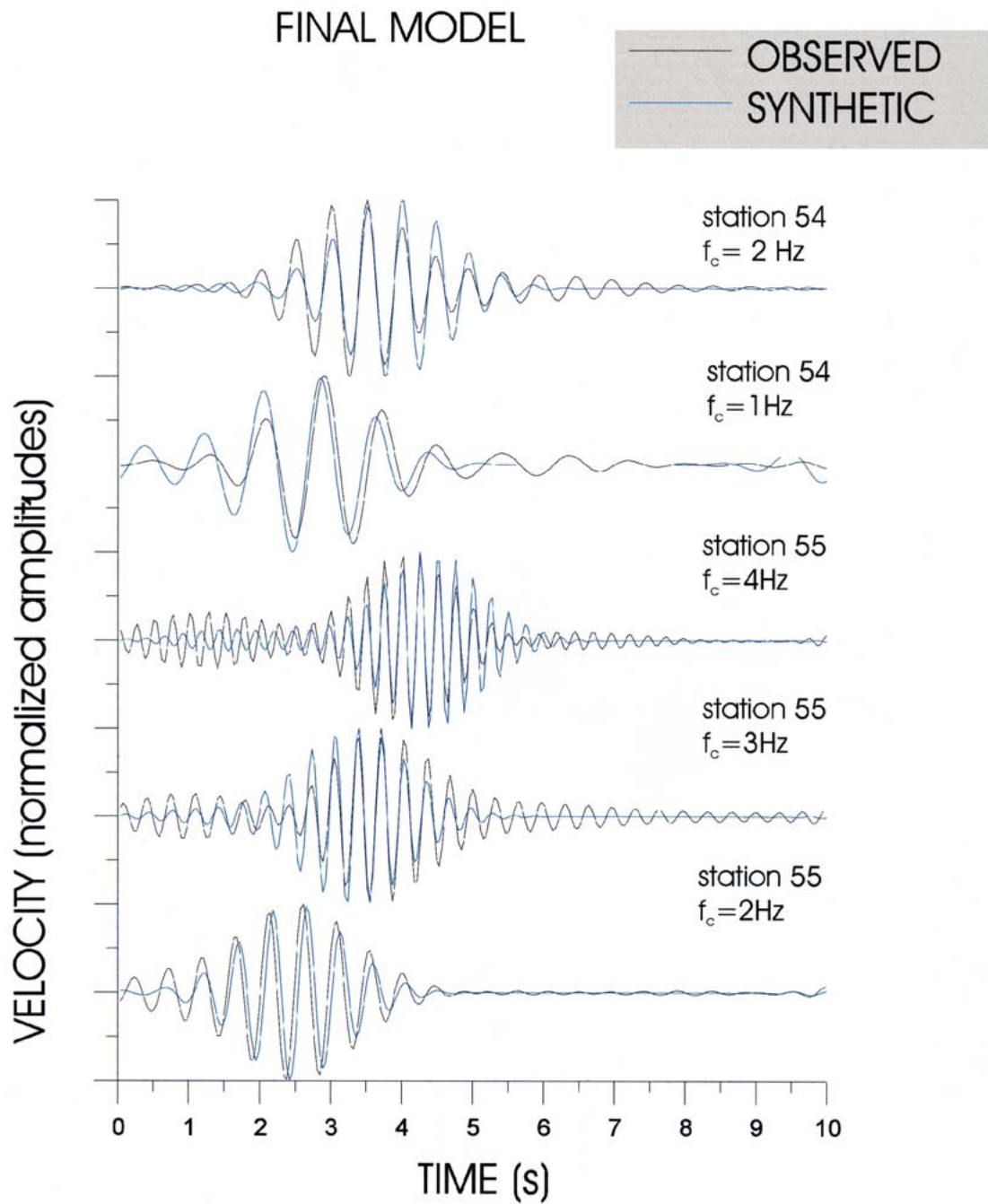


Figure 7. Comparison between the observed gaussian-filtered seismograms (black line) and corresponding synthetic filtered traces (blue line). The velocity model used to compute the synthetic wave field is the final model (see the text).

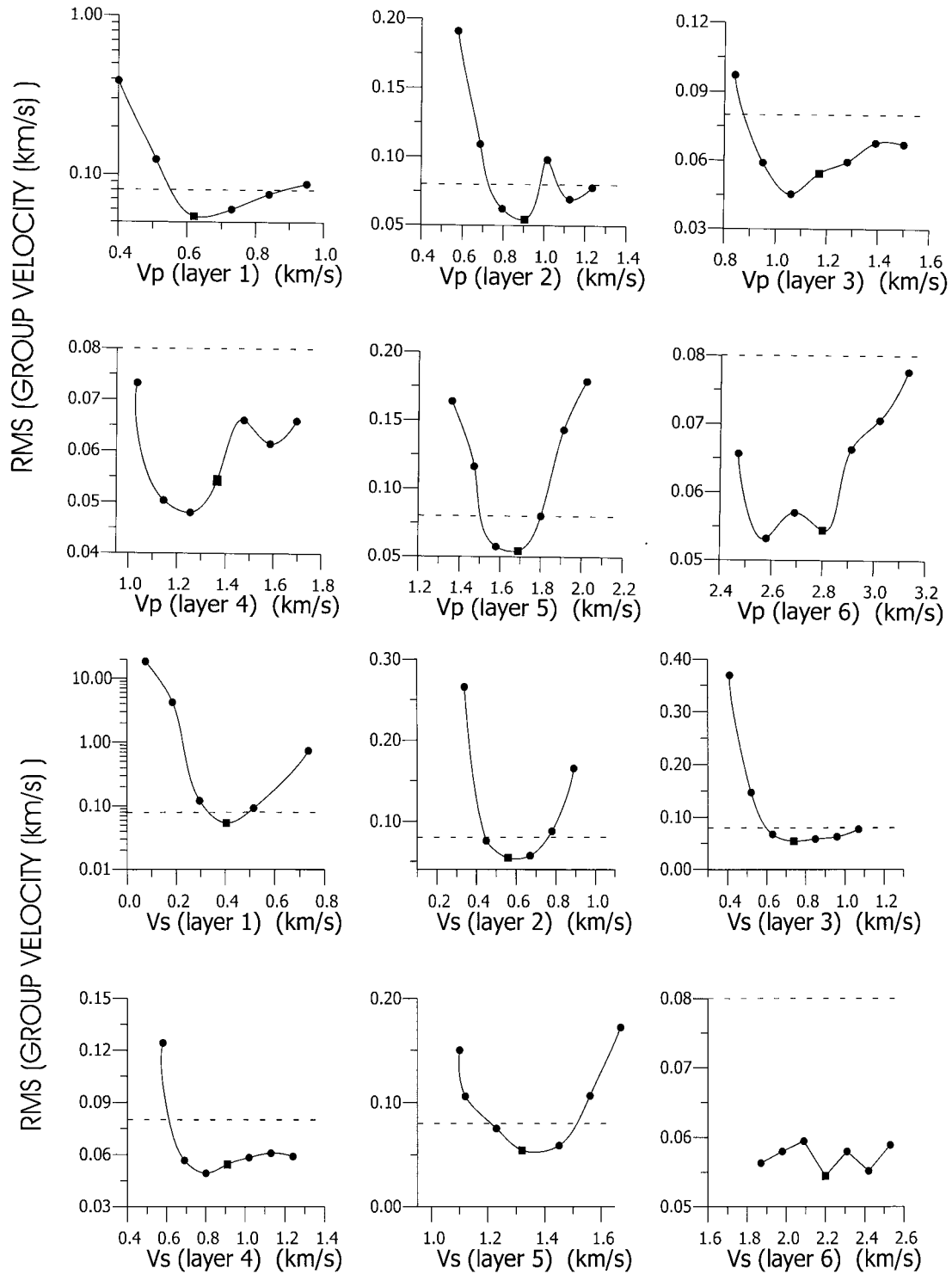


Figure 8. (a) – Representation of the misfit between observed and theoretical group velocities as a function of V_p of each layer. The circles represent the computed values. The square refers to the retrieved velocity model (Table 2). The shaded line in each graph represents the 1σ standard deviation. (b) – The same as in a) but for V_s values.

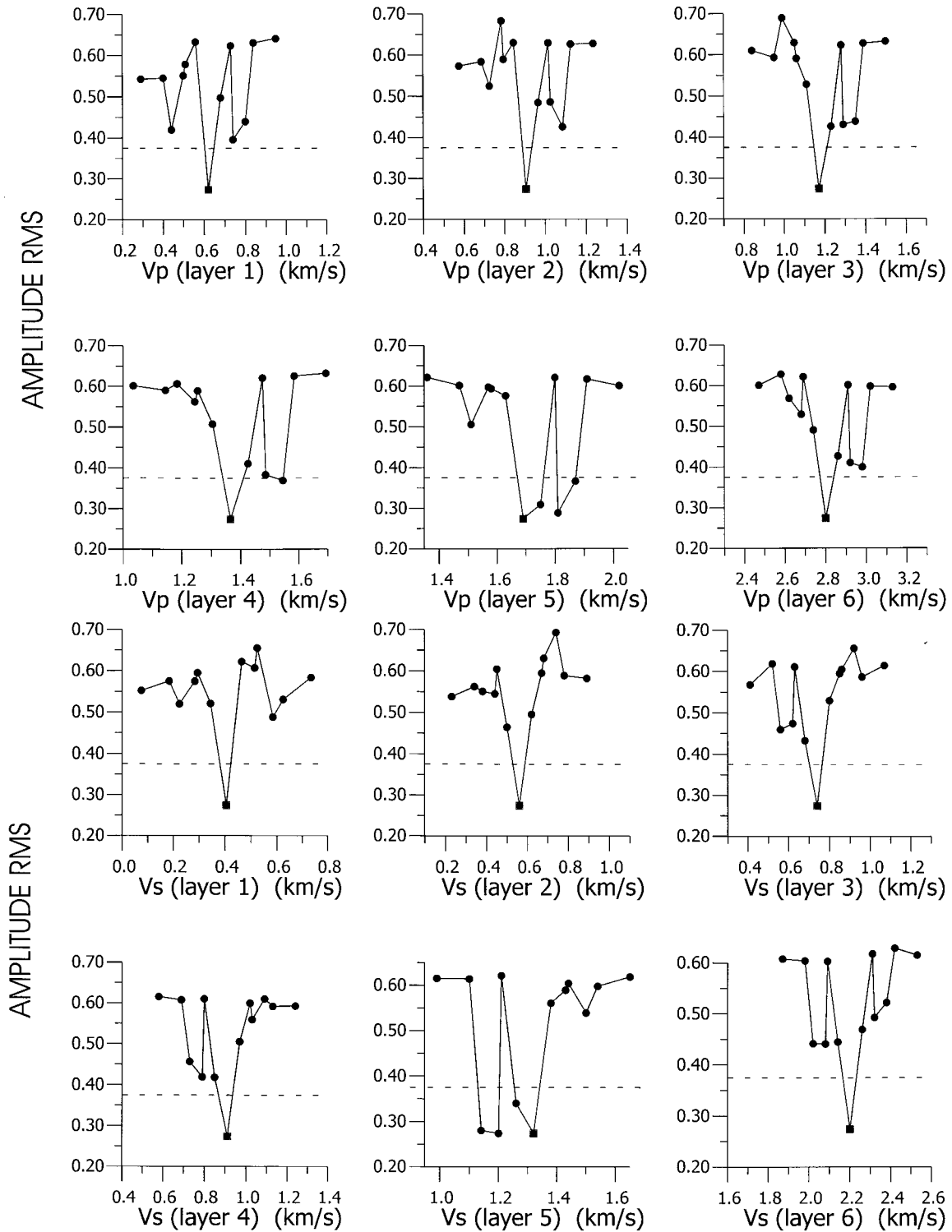


Figure 9. (a) – Representation of the misfit between observed and theoretical amplitudes as a function of Vp of each layer. The circles represent the computed values. The square refers to the retrieved velocity model (Table 2). The shaded line in each graph represents the 1σ standard deviation. (b) – the same as in a) but for Vs values of each layer.

(here assumed equal to 5% of the maximum observed amplitude), the estimated average error on amplitude data results equal to $\langle \Delta A \rangle = 0.375$. $\langle \Delta A \rangle$ is non-dimensional since we used normalized traces. The fixed threshold allows us for a total number of available amplitude data equal to 352.

Following the same lines of the previous section, we computed the r.m.s. misfit function between theoretical and observed amplitudes for different values of the body wave velocity of each layer around the Vp and Vs values of the obtained velocity model (Table 2). In Figure 9 the resolution analysis based on amplitude data is shown. The r.m.s. is obtained by averaging the r.m.s. of each of the five couples of considered seismograms, by using the following relationship:

$$r.m.s. = \sqrt{\frac{\sum_{i=1}^N (A_{obs,i} - A_{teo,i})^2}{N}}$$

where $A_{obs,i}$ represents the i -th amplitude data and $A_{teo,i}$ represents the i -th amplitude measured on the corresponding synthetic seismogram. Results can be summarized in the following way (Figure 9):

1. both Vp and Vs model parameters of each layer (both in the shallow layer and in the halfspace) are well resolved.
2. The level of uncertainties affecting model parameters is always less than 0.05 km/sec.

We retain that the reason for the very high difference of results, arising from the two resolution analysis, is due to the different number of data considered. In fact, in the first approach we used only 17 data (all the group velocity data of the dataset). In the second analysis, based on amplitudes, the starting number of considered data was 5(number of seismogram) time 128 (number of point of each seismogram), that was successively reduced to 352 by introducing a threshold equal to 5% of maximum amplitude on each seismogram. The enormous increase of the number of available data in the amplitude analysis reflects in its higher resolving power, although its local character (i.e. between P54 and P55 stations).

Discussion and conclusions

The modeling of the dispersion curves of group velocity of Rayleigh waves and the next optimization of the semblance between some high quality filtered data and the corresponding synthetics aimed us to infer:

- the range of variability of body wave velocities in the studied area (the starting model)
- and a more refined but local velocity model of the sediments in the zone of the Sannio region located between P54 and P55 stations.

The first result we point out consists of the observation of very high gradients both in Vp and in Vs velocities in going from the surface to the base of the so-called bedrock (the layer below the depth of 150 m). Both Vp and Vs near triplicate their value in going from zero m of depth to 80 m of depth. Thus the shallow sedimentary layer in the area could act as a guide that traps the energy traveling into it. Owing to the seismogenetic potential of the Sannio area a further study is need to evaluate the role played by the inferred shallow high velocity contrast on site effects.

The second important result consists of the low Vp/Vs ratio (ranging from 1.5 and 1.7) for the first 5 layers of the inferred model (the shallow sediments). This result should indicate that, at least between the P54 and P55 stations, sediments should be strongly compacted.

With increasing depth, resolution in our Vp and Vs estimates strongly deteriorates; this is primarily due to the interference between the Rayleigh waves and the P waves. However the two station analysis seems indicate only a slight reduction in P-wave velocity (2.8 km/s) with respect to the average values determined by Iannaccone et al. (1998) (3 km/s).

The applied technique shows that surface waves recorded on active seismic profiles can be very useful to constrain the velocity of superficial layers which are poorly determined by arrival time modeling; in particular, the use of amplitude variations of Rayleigh waves around their group velocity peak allows for an enormous increase of Vp and Vs resolution.

The lack of instrumental calibration curves prevented attenuation analysis based on calculation of differential seismograms as described in recent papers (see e.g. Du and Foulger, 1999; and references therein).

Acknowledgements

Signal processing of the seismograms was performed with the PITSA software developed by R. Scherbaum. Complete wave field analysis was performed using a modified version of the computer program AXITRA, written by O. Coutant.

References

- Bard, P.Y. and Bouchon, M., 1985, The two-dimensional resonance of sediment-filled valleys, *Bull. Seism. Soc. Am.* **75**, 519–541.
- Bouchon, M., 1979, Discrete wave-number representation of elastic wave fields in three-space dimensions, *J. Geoph. Res.* **84**, 3609–3614.
- Bouchon, M., 1981, A simple method to calculate Green's functions for elastic layered media, *Bull. Seism. Soc. Am.* **71**, 959–971.
- Du, Z.J. and Foulgers, G.R., 1999, The crustal structure beneath the northwest fjords, Iceland, from receiver functions and surface waves, *Geoph. J. Int.* **139**, 419–432.
- Dunkin, J.W., 1965, Computation of model solutions in layered, elastic media at high frequencies, *Bull. Seism. Soc. Am.* **55**, 335–358.
- Dziewonski, A.M. and Hales, A.L., 1972, Numerical analysis of dispersed seismic waves, In: Bolt, B.A. (ed.), *Methods of Computational Physics 11: Seismology: Surface waves and Earth Oscillations*, Academic Press, New York and London, 309 pp.
- Harkrider, D.G., 1964, Surface waves in multilayered media. I. Rayleigh and Love waves from buried sources in a multilayered elastic half-space, *Bull. Seism. Soc. Am.* **54**, 627–679.
- Haskell, N.A., 1953, The dispersion of surface waves on multilayered media, *Bull. Seism. Soc. Am.* **43**, 17–34.
- Iannaccone, G., Improta, L., Capuano, P., Zollo, A., Biella, G., De Franco, R., Deschamps, A., Cocco, M., Mirabile, L. and Romeo, R., 1998, A P-wave velocity model of the upper crust of the Sannio region (Southern Apennines, Italy), *Ann. Geof.* **41**, 567–582.
- Improta, L., Iannaccone, G., Capuano, P., Zollo, A. and Scandone, P., 2000, Inferences on the upper crustal structures of Southern Apennines (Italy) from seismic refraction investigations and subsurface data, *Tectonophys.* **317**, 273–297.
- Kennett, B.L.N., 1983, *Seismic wave propagation in stratified media*. Cambridge University Press, Cambridge.
- Knopoff, L., 1961, Green's function for eigenvalue problems and the inversion of Love wave dispersion data, *Geoph. Journ.* **4**, 161–173.
- Lee, W.H.K. and Stewart, S.W., 1981, Principles and Applications of Microearthquake Networks, In: Saltzman, B. (ed.), *Advances in Geophysics*, Supplement 2, Academic Press, Inc. (London), London, 293 pp.
- Malagnini, L., Hermann, R.H., Mercuri, A., Opice, S., Biella, G. and de Franco, R., 1997, Shear-wave velocity structure of sediments from the inversion of explosion-induced Rayleigh waves: comparison with cross-hole measurements, *Bull. Seism. Soc. Am.* **87**, 1413–1421.
- Muller, G., 1985, The reflectivity method: a tutorial, *J. Geophys.* **58**, 153–174.
- Nolet, G., 1990, Partitioned waveform inversion and two-dimensional structure under the Network of Autonomously Recording Seismograms, *J. Geophys. Res.* **95**, 8499–8512.
- Press, W.H., Flannery, B.P., Teukolsky, S. A., and Vetterling, W.T., 1994, *Numerical Recipes*, Cambridge University Press, New York.
- Sambridge, M.S. and Drijkoningen, G., 1992, Genetic algorithms in seismic waveform inversion, *Geoph. J. Int.* **109**, 323–342.
- Telford, W.M., Geldart, L.P., Sheriff, R.E. and Keys, D.A., 1990, *Applied Geophysics*. 2nd edn. Cambridge University Press, Cambridge.
- Yao, P.C. and Dorman, J., 1992, Short period surface wave dispersion and shallow crustal structure of central and eastern Tennessee, *Bull. Seism. Soc. Am.* **82**, 962–979.